Research Square

Preprints are preliminary reports that have not undergone peer review.
They should not be considered conclusive, used to inform clinical practice,
or referenced by the media as validated information.

Evaluation of two different 3D electrodes in the electrogenerative removal of tin(II) from chloride solutions using a flow-through reactor

Jehad M. Al Issa
Jerash University
Samer S. Aburub
Philadelphia University
Alaa A. Al-Akhras
Jerash University
Wasan Hussien Alkassabeh
Universiti Sains Malaysia
Ali O. Alqarni
Najran University
Faiz Bukhari Mohd Suah
fsuah@usm.my

Universiti Sains Malaysia

Article

Keywords: Carbon felt, Electrogenerative, Flow-through reactor, Reticulated vitreous carbon, Tin removal

Posted Date: November 18th, 2026

DOI: https://doi.org/10.21203/rs.3.rs-11558571/v1

License: This work is licensed under a Creative Commons Attribution 4.0 International License.
Read Full License

Additional Declarations: No competing interests reported.

Evaluation of two different 3D electrodes in the electrogenerative removal of tin(II) from chloride solutions using a flow-through reactor

Jehad M. Al Issa[*,a], Samer S. Aburub[b], Alaa A. Al-akhras[a], Wassan Hussien Alkassabeh[c], Ali O. Alqarni[d] and Faiz Bukhari Mohd Suah[*,e]

[a] Chemistry Department, Faculty of Science, Jerash University, Jerash, 26150, Jordan.

[b] Applied Chemistry Department, Faculty of Science, Philadelphia University, Amman, 19392, Jordan

[c] Discipline of Clinical Pharmacy, School of Pharmaceutical Sciences, Universiti Sains Malaysia, Pulau Pinang 11800, Malaysia

[d] Department of Pharmaceutical Chemistry, College of Pharmacy, Najran 11001, Najran University, Saudi Arabia

[e] Green Analytical Chemistry Laboratory, School of Chemical Sciences, Universiti Sains Malaysia, 11800 Pulau Pinang, Malaysia

* Corresponding authors: fsuah@usm.my*, jehadissa97@gmail.com*

Abstract

This study investigates the electrogenerative removal of tin(II) from $SnCl_2$/NaCl solutions using carbon felt (CF) and reticulated vitreous carbon (RVC) cathodes coupled to a sacrificial zinc anode in a flow-through reactor. Cyclic voltammetry on CF showed a cathodic wave and an anodic stripping peak attributable to Sn(II)/Sn(0) deposition and dissolution, superimposed on hydrogen evolution at negative potentials. The influence of the cathode material, initial Sn(II) concentration, dissolved oxygen and pH were examined. With 500 mg L−1 of Sn(II), CF and RVC removed 99.6% and 98.6% of the dissolved Sn(II) concentration, respectively, after 4 h. CF performed slightly better than RVC at all sampling times, but the differences (1-4 percentage points) were within the experimental scatter. Nitrogen purging increased the 4 h removal from 82.3 % to 99.6 %, and removal was faster at pH 7 than at pH 4 or 5. The concentration decay followed apparent pseudo-first-order rather than zero-order kinetics (k_1 = 1.35 h^{-1} for CF and 1.07 h^{-1} for RVC), but the strong dependence of the rate on dissolved

oxygen and pH indicates that the process was not controlled by mass transport alone. Scanning electron microscopy showed a cracked deposit on the CF fibres. Because the cell current, the tin mass balance and the composition of the deposit were not determined, the results establish efficient removal of dissolved Sn(II) but not the faradaic efficiency or the purity of the recovered tin; these quantities are identified as priorities for further work.

Keywords: Carbon felt; Electrogenerative; Flow-through reactor; Reticulated vitreous carbon; Tin removal.

1. Introduction

Tin (Sn) is a Group 14 element of the carbon family and a soft, silvery-white metal. It has been used since antiquity, mainly as a component of bronze, a copper–tin alloy. Sn is used to coat steel cans commonly used as food containers, and also as a bearing and welding metal (Reijnders, 2016).

Metals can be recovered using a variety of methods, including hydrometallurgy and pyrometallurgy. Electrogenerative recovery involves metal deposition driven by a spontaneous galvanic reaction without an externally applied voltage (Roslan et al., 2017). In the present system, zinc oxidation supplies electrons through an external circuit for Sn(II) reduction at a separate CF or RVC cathode. The process is based on the galvanic principle, rather than the externally powered electrolytic electrodeposition (Flowers et al., 2019) .The separated electrodes are what distinguish this configuration from direct-contact cementation.

An electrogenerative system has been previously suggested as a viable alternative to traditional recovery methods. Among the electrodes tested, CF and RVC cathode materials have been shown to be the most effective, which recovered more than 99% of Au(III) in just one hour of operation (Roslan et al., 2017). CF is characterised by its large surface area and porosity, which enable it to offer numerous redox reaction sites. These properties contribute to

high electrolytic efficiency and mechanical stability, all while maintaining a reasonable cost, making CF an attractive electrode material for electrogenerative applications (Tichter & Marshall, 2022). CF was frequently utilised as a cathode material in the electrofusion process to remove persistent organic pollutants (POPs) from aqueous medium (Le et al., 2017).

An electrode is a critical component of the devices that provides the surface area for the reaction to occur in the electrogenerative system. The structure of these electrodes is essential in the process because it determines the ease of electrolyte flow through the electrode, electrical conductivity, and structural stability (Chakrabarti et al., 2014). The RVC, which possesses appealing properties such as a microporous honeycomb structure and glassy carbon electrode material, has the potential to be used in innovative electrochemical cell designs. It offers high current densities, low electrical resistance, and high electrical conductivities as an electrode, in addition to having a strong corrosion resistance with good porosity and a large surface area (Mansor et al., 2019).

Recent studies illustrate the growing use of carbon-based electrodes in metal removal, including interface-engineered carbon felt for capacitive uranium removal (Zhang et al., 2026), solar-driven ZnS@MXene/CF cathodes (Liu et al., 2025), and self-bias photocatalytic systems combining uranium removal with electricity generation (Cao et al., 2026). These studies point to the importance of electrode interfaces and charge transfer for enhanced performance. Motivated by a general interest on carbon-based electrodes, the present work considers CF and RVC for Sn(II) recovery in a flow-through reactor driven by Zn oxidation.

In electrogenerative reactors, an ion exchange membrane is used to separate the anolyte and catholyte solutions and it is important that these solutions differ in concentration. This type of separation enables selectivity improvement in the ion charge transfer between the two compartments, which is necessary for efficient electrochemical reactions. A. Ion-exchange membranes Two major types of ion-exchange membranes exist. Anion exchange membranes

allow the passage of negatively charged ions, while cation exchange membranes allow the passage of positively charged ions (Kumar et al., 2013).

Different mechanisms and products are involved in different tin recovery methods. Acid leaching dissolves tin from the solid waste for further recovery (Jha et al., 2012). The dissolved tin is removed by chemical precipitation as a solid compound and may be affected by complexing agents (Thomas et al., 2018). More recently, selective Sn(IV) adsorption in acidic solutions (Wang et al., 2024) and deep eutectic solvents for indium–tin separation from spent LCDs (Wang et al., 2025) were reported. These separation methods typically require additional processing to isolate the metallic tin. Conventional electrolytic electrodeposition uses an external power supply, whereas electrogenerative recovery couples metal-ion reduction with sacrificial-anode oxidation, without an externally applied voltage (Mansor et al., 2019; Roslan et al., 2017). Mohd Azhari et al. (2024) have already investigated this approach for Sn(II) using CF and a zinc anode in a batch cell. Building on that work, the present study compares CF and RVC under identical flow-through conditions. Its contribution lies in this comparative evaluation, while any energy or environmental advantages require assessment of zinc consumption, pumping requirements, and product recovery.

2. MATERIALS AND METHODS

2.1 Chemicals and materials

Analytical grade chemicals, such as tin(II) chloride ($SnCl_2$) (99.8 %, Sigma), sodium hydroxide (NaOH) (99 %, QRëC), nitric acid (HNO_3) (65 %, QRëC), ethanol, concentrated sulphuric acid (H_2SO_4) (95 %, QRëC), and concentrated hydrochloric acid (HCl) (37 %, QRëC) were used in this study. Sodium chloride (NaCl) (99.8 %) was obtained from Bendosen. In the study, the following materials and electrode configurations were used. A Neosepta® AM-01 anion exchange membrane, supplied by Tokuyama Corporation, was used, which is designed

to allow the selective passage of anions while preventing mixing of the anolyte and catholyte solutions.

The anode was composed of pure zinc foil (R&M) measuring 1.9 cm × 4.7 cm × 0.05 cm, serving as the electrode for oxidation reactions. For the cathode, two materials were used: CF (MonotaRO Co., Ltd.) with dimensions 1.9 cm × 4.7 cm × 0.5 cm, and RVC with 30 pores per inch (The Electrosynthesis), also measuring 1.9 cm × 4.7 cm × 0.5 cm.

A platinum wire was used as the counter electrode and an Ag/AgCl reference electrode (RE-5B, Bioanalytical Systems) as the reference electrode for the cyclic voltammetry measurements. All potentials are reported versus this electrode. For sample analysis, a standard tin solution at 1000 mg L^{-1} was prepared and diluted to appropriate concentrations to quantify tin recovery effectively.

The described flow-through electrogenerative system consists of several key components designed for the efficient recovery of tin. Two 250 mL beakers are used as reservoirs for the anolyte and catholyte solutions, respectively, keeping them separate and under controlled conditions in each half-cell. The electrolyte solutions were pumped through the system at a constant flow rate of 50 mL min^{-1} using a peristaltic pump to keep the system under steady-state conditions and to provide mass transfer. The cell voltage and current were monitored using a Sanwa digital multimeter, but these values were not logged for the experiments reported here.

The galvanic cell consists of two compartments: one for the anolyte and one for the catholyte. These compartments are placed on opposite sides of an anion exchange membrane, which physically separates the solutions but allows selective ion transfer. The setup includes stainless-steel end plates that hold the membrane and electrodes in place, sandwiched between Teflon plates that provide chemical resistance. Each electrolyte chamber, with dimensions of 6.5 cm × 1.5 cm × 1.0 cm, was positioned between two mesh flow frames serving as turbulence

promoters, which improve electrolyte flow and promote uniform reaction conditions. Figure 1 visually shows the complete setup of this flow-through electrogenerative cell.

Each electrolyte was recirculated in a separate closed loop between its 250 mL reservoir and its compartment at 50 mL min^{-1} (0.83 cm^3 s^{-1}), entering at the bottom of the compartment and leaving at the top. The empty volume of each compartment is 9.75 cm^3 (6.5 cm × 1.5 cm × 1.0 cm). On an empty-compartment basis, the mean hydraulic residence time in the cathode compartment was therefore about 11.7 s, and the mean superficial velocity along the 6.5 cm flow path (cross-section 1.5 cm^2) was about 0.56 cm s^{-1}. Because the porous cathode (4.47 cm^3) and the mesh flow frames occupy part of the compartment, the actual interstitial velocity was higher and the residence time shorter than these values. The catholyte reservoir was turned over once every 5 min, corresponding to about 48 passes through the cell during a 4 h experiment.

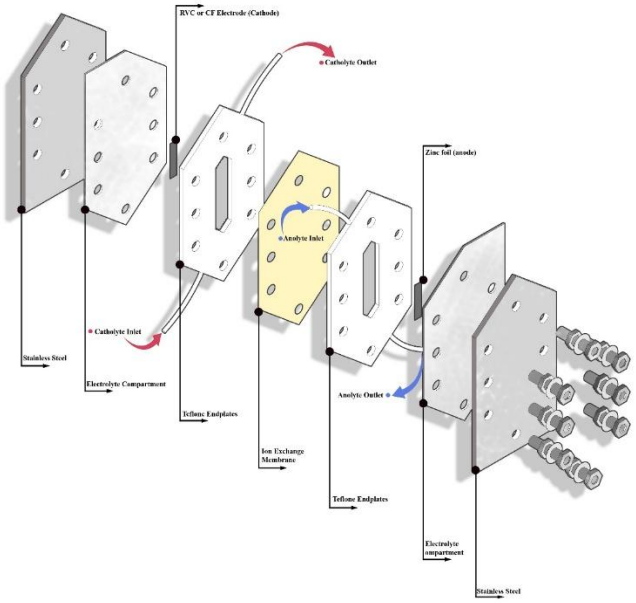


Figure 1. Schematic diagram of the flow-through electrogenerative cell.

The catholyte and anolyte solutions can enter and exit the cell at designated points. The cell is fastened to the base with eight bolts and nuts to prevent leakage, while a peristaltic pump (Masterflex) draws electrolytes in through the bottom inlet and discharges them from the top outlet. When the circuit is closed, the anolyte and catholyte regions each receive their own supply of electrolytes. The anode is a sheet of zinc metal, while the current collector is made of stainless steel. An external conductive wire was used to connect the current collectors to complete the circuit.

All the electrolytes were prepared using analytical-grade ingredients. Distilled deionised water and 0.2 M NaCl were used to prepare catholyte solutions with varying concentrations of Sn(II). The 0.1 M and 0.2 M NaCl solutions for the anolyte and catholyte were prepared by adding appropriate amounts of NaCl to 1 L volumetric flasks and diluting them with distilled water. Sn(II) solutions at concentrations of 50, 100, 250, and 500 mg L^{-1} were prepared in 0.2 M NaCl, and 250 mL of each solution was used as the catholyte. The pH was adjusted to 7 by carefully adding 0.1 M HCl or 0.1 M NaOH to the volumetric flask until the target value was reached.

2.2 Electrodes

In the experimental setup, CF and RVC are used as cathode materials. The anode was a pure zinc foil which was polished with coarse sandpaper prior to use to remove surface oxidation and maintain good electrical conductivity. These measures aimed to keep the electrode surfaces clean and reactive, thus improving the efficiency of tin recovery during the electrochemical process. Table 1 gives the details and features of the electrodes used in the experiments.

Table 1. Experimental conditions of the anode and cathode Channels

	Anode		Cathode
Anolyte	250 mL of a 0.1 M NaCl solution	Catholyte	Sn(II) in 0.2 M NaCl (50, 100, 250, 500) mgL^{-1}
Anode	Zinc foil 99%	Cathode	RVC or CF

(1.9 cm × 4.7 cm × 0.05 cm)	(1.9 cm × 4.7 cm × 0.5 cm)

The cathodes were pre-treated before analysis. The cathode was first immersed in a 95:5 mixture of ethanol and ultra-pure water for 4 h to remove organic impurities and improve the surface moisture properties. Then the cathode was washed with distilled water and then soaked in H 2 SO 4 for another 4 h. Then it was rinsed with distilled water to keep it moist and kept in ultra-pure water.

2.3 Tin recovery experiment

Each experiment used 250 mL of anolyte (0.1 M NaCl) and 250 mL of catholyte (Sn(II) in 0.2 M NaCl), each held in its own reservoir. Circulation of the anolyte was started first; the catholyte was then pumped into the cathode compartment, and both streams were recirculated separately at 50 mL min^{-1} throughout the experiment. The anode and cathode current collectors were connected directly by an external wire without an additional load, so the cell operated under short-circuit conditions. To evaluate the system's performance in terms of Sn(II) removal, the remaining Sn(II) concentration in the catholyte was measured at set intervals by UV–vis spectrophotometry over 4 h, using calibration standards prepared by diluting the 1000 mg L^{-1} Sn standard solution (Section 2.1). The percentage removal of Sn(II) was calculated using Eq. (1):

$$\text{Sn(II) removal (\%)} = \frac{C_0 - C_t}{C_0} \times 100 \quad (1)$$

where C_0 is the initial Sn(II) concentration and C_t is the Sn(II) concentration at sampling time t (both in mg L^{-1}). To determine the remaining tin in solution, 10 mL of the catholyte was taken after 30 minutes, 1, 2, 3, and 4 hours. Sampling therefore removed 50 mL in total (20 % of the initial catholyte volume). Because Eq. (1) is based on concentrations, it is not affected directly by this volume change; the change was taken into account in the kinetic analysis (Section 2.6). Eq. (1) quantifies the decrease of dissolved Sn(II) in the catholyte, i.e. its removal

from solution, and does not by itself show which fraction of the removed tin was deposited on the cathode.

This method also investigated the effects of the cathode material, the initial Sn(II) concentration, nitrogen purging and the catholyte pH. Each experiment was performed three times, and mean values are reported. The morphology of the CF cathode before and after operation was examined by scanning electron microscopy (SEM); the micrograph after operation was recorded with a TESCAN VEGA 3 microscope.

2.4 Cyclic Voltammetry (CV) Analysis

Cyclic voltammetry (CV) was employed to study the redox behaviour of Sn(II) ions and evaluate the electrochemical response of the CF electrode. The measurements were carried out using a standard three-electrode setup comprising a CF working electrode, a platinum wire as the counter electrode, and an Ag/AgCl reference electrode. Test solutions containing Sn(II) at concentrations of 250 mg L^{-1} and 500 mg L^{-1} were prepared in 0.2 M NaCl. The potential was scanned from –1800 mV to +2000 mV at a rate of 100 mV s^{-1} using a PalmSens potentiostat. All measurements were performed at ambient temperature. In the voltammograms, cathodic currents are plotted as positive values. The wide potential window was chosen to include both the deposition of tin and its anodic stripping; because it also includes hydrogen evolution and anodic reactions of the electrolyte and the carbon surface, the voltammograms were interpreted with reference to the standard potentials of the relevant couples.

2.5 Effect of pH on Tin Recovery

To evaluate the effect of pH on Sn(II) removal, the pH of the catholyte was adjusted to specific values (pH 4, 5, and 7), while a non-controlled condition was also included, in which

the freshly prepared $SnCl_2$/NaCl solution was used at its natural pH. This pH is acidic because of Sn(II) hydrolysis; its value was not recorded. pH adjustments were carried out using 0.1 M HCl or 0.1 M NaOH prior to the start of each experiment. All tests were performed using 500 mg L^{-1} Sn(II) solutions under consistent operational parameters. Tin concentrations were measured at designated time intervals over a 4-hour period by UV–vis spectrophotometry to determine the removal at each pH.

2.6 Data analysis

Removal–time data were evaluated with the zero-order model ($C_t = C_0 - k_0 t$) and the pseudo-first-order model ($\ln(C_t/C_0) = -k_1 t$) by least-squares regression of the mean values of the three runs; the pseudo-first-order fit was constrained through the origin, as required by Eq. (6) (Section 3.6), and the coefficient of determination (R^2) is reported for both models. The apparent product of the mass-transfer coefficient and the specific electrode area, $k_m A_e$, was obtained from Eq. (6) using the actual catholyte volume in each sampling interval (250 mL before the first sample, decreasing by 10 mL after each sample). The charge required to reduce the Sn(II) removed from solution was calculated from Faraday's law, $Q = nF\Delta m_{Sn}/M_{Sn}$, with n = 2, F = 96 485 C mol^{-1} and M_{Sn} = 118.71 g mol^{-1} (Bard & Faulkner, 2001). In Figs. 3, 5 and 8, the error bars correspond to ±5 % of each plotted value. Because the individual replicate values were not available, formal significance tests could not be performed; differences smaller than the error bars are therefore not interpreted as significant.

3. RESULTS AND DISCUSSION

3.1 Electrogenerative process

The electrochemical deposition of Sn on the surface of the electrodes is based on the electrogenerative process. The reactions occurring during the electrogenerative process are outlined in the following equations:

Anode: $Zn_{(s)} \leftrightarrows Zn^{2+}{}_{(aq)} + 2e^-$ E^o_{ox}= + 0.76 V (2)

Cathode: $Sn^{2+}{}_{(aq)} + 2e^- \leftrightarrows Sn_{(s)}$ E^o_{red}= - 0.14 V (3)

Overall : $Zn_{(s)} + Sn^{2+}{}_{(aq)} \leftrightarrows Zn^{2+}{}_{(aq)} + Sn_{(s)}$ E_{cell} = + 0.62 V (4)

Using standard reduction potentials of −0.14 V for Sn^{2+}/Sn and −0.76 V for Zn^{2+}/Zn, the standard cell potential is E°cell = −0.14 − (−0.76) = +0.62 V. Accordingly, ΔG° = −nFE°cell ≈ −119.6 kJ mol^{-1}, with n = 2. These calculated values are reflective of the thermodynamic favourability under standard conditions, they are not a measured quantity under the experimental conditions. Ecell,eq = E°cell − (RT/2F) ln[a(Zn^{2+})/a(Sn^{2+})] under experimental conditions, where an is free-ion activity (Flowers et al., 2019). Namely, the formation of Sn(II) chloro-complexes can modify the activity of free Sn^{2+}, and thus the total dissolved Sn(II) concentration should not be directly substituted for the free-ion activity in the Nernst equation. The operating current is affected by polarization, resistance and mass transport. Under short-circuit conditions, the terminal voltage is close to zero despite the chemical driving force.

$\Delta G^\circ = -nFE^\circ{}_{cell}$ (5)

The cell current was not recorded during the experiments, so the charge passed and the faradaic efficiency of Sn deposition could not be determined directly. The charge that the observed removal would require can nevertheless be estimated. The catholyte initially contained 125 mg of Sn (500 mg L^{-1} × 0.25 L, i.e. 1.05 mmol), whose complete reduction to Sn(0) requires 203 C, corresponding to an average current of about 14 mA over 4 h. However, 77 % of the Sn(II) was removed in the first 30 min with CF (Fig. 3); if this removal were entirely due to electrodeposition, it would require an average current of about 87 mA during this period. Whether the galvanic cell delivered such a current, or whether part of the initial removal occurred by other routes (Sections 3.6 and 3.7), cannot be established from the present data. The stoichiometric zinc consumption for complete Sn deposition is 0.551 g Zn per g Sn

(68.8 mg Zn for 125 mg Sn), which is small compared with the mass of the zinc foil (about 3.2 g). The cell was operated at short circuit and thus the terminal voltage and the useful power output of the cell were close to zero. Therefore, the process should be assessed as a recovery method rather than a power source.

3.2 Cyclic voltammetry (CV) analysis

CV analysis was performed to study the electrochemical behavior of the cathodes and to monitor electron transfer reactions in the system. This technique is of key importance in electrochemistry, as it permits the identification of reduction and oxidation processes in molecular species, as well as other reactions driven by electron transfer, including catalytic activity. It is also a quick and reliable method to determine redox potentials of electroactive species. CV tests were performed in this work with Sn(II) solutions of 250 mg L^{-1} and 500 mg L^{-1} using a CF electrode to study the redox properties of Sn(II) and to evaluate the effect of chloride ions on tin recovery.

For the 250 mg L^{-1} Sn(II) solution, the potential was scanned from –1800 mV to +2000 mV at a rate of 100 mV s^{-1}. For this solution (Fig. 2, curve a), the most distinct feature was a cathodic peak at about +0.36 V (≈2.0 mA), and no distinct anodic stripping peak was observed in the region expected for Sn(0) oxidation. In the 500 mg L^{-1} Sn(II) solution, the voltammogram (curve b) displayed a cathodic shoulder near −1.2 V, superimposed on the rising cathodic current, and a well-defined anodic peak at about −0.35 V (≈0.8 mA). The large cathodic currents at the most negative potentials and the large anodic currents positive of about +1.3 V are attributed mainly to hydrogen evolution and to chloride and water oxidation, respectively.

The standard potential of the Sn^{2+}/Sn couple (−0.14 V vs. SHE; Bard & Faulkner, 2001) corresponds to approximately −0.35 V vs. Ag/AgCl. The anodic peak at −0.35 V for 500 mg L^{-1} Sn(II) is therefore assigned to the stripping of tin deposited during the cathodic scan, and

the cathodic shoulder near −1.2 V to Sn(II) reduction. The large separation between deposition and stripping reflects the nucleation overpotential of tin on carbon and the ohmic drop in the porous electrode; in addition, complexation of Sn(II) by chloride and hydroxide shifts its reduction negative of the value calculated for free Sn^{2+} (Séby et al., 2001; Cigala et al., 2012). The cathodic peak at +0.36 V observed for 250 mg L^{-1} lies far positive of the Sn^{2+}/Sn potential and cannot be due to Sn(II) reduction to the metal; it may arise from the reduction of species generated at the positive end of the scan, such as Sn(IV) (Sn(IV)/Sn(II): +0.15 V vs. SHE, about −0.06 V vs. Ag/AgCl) or oxidised chlorine species, but it cannot be assigned unambiguously because no blank voltammogram was recorded. The CV results therefore show that Sn(II) is reduced on CF and that the deposit can be re-oxidised, but they do not quantify the deposition efficiency.

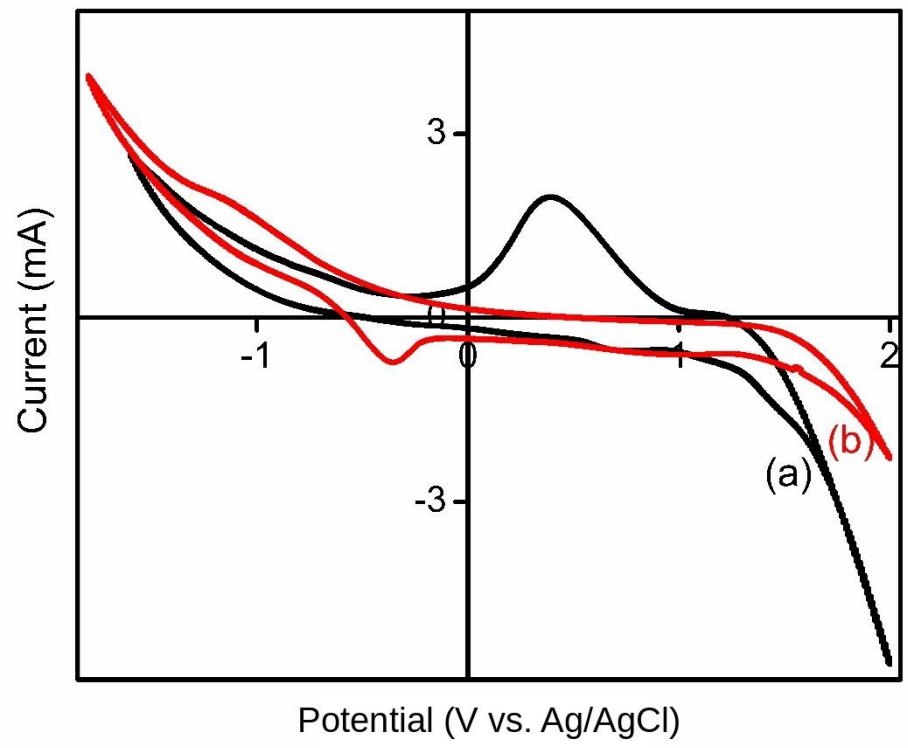


Figure 2. Cyclic voltammograms for CF cathode with (a) 250 mg L^{-1} Sn(II) and (b) 500 mg L^{-1} Sn(II) in 0.2 M NaCl at 100 mV s^{-1}; potentials vs. Ag/AgCl; cathodic currents are plotted as positive values.

3.3 Effect of different cathode materials

CF and RVC were compared as cathodes for the electrogenerative removal of Sn(II) in the flow-through cell. By using 500 mg L^{-1} of Sn(II) initially with CF as the cathode material, the removal reached 77.1 % after 30 min and 99.6 % after 4 h (Fig. 3), compared with 75.0 % and 98.6 % with RVC. CF gave slightly higher mean removal at every sampling time, but the differences (1.0–4.1 percentage points) were smaller than the error bars, so the two cathodes performed similarly under the conditions tested.

The slightly faster removal with CF, which is also reflected in its higher apparent k_mA_e (Section 3.6), is consistent with the structural differences between the two materials. CF consists of a fibrous, highly porous network, whereas RVC has a rigid open-cell vitreous carbon skeleton whose specific surface area depends on its pore grade (Friedrich et al., 2004). These differences could give CF more sites for tin nucleation and growth and a different flow distribution through the electrode.

However, although the two cathodes had the same geometric volume (4.47 cm^3), they may differ substantially in mass, real surface area, pore architecture, electrical conductivity and hydrodynamic resistance, none of which was measured in this study. Normalisation by geometric volume does not change the comparison, and normalisation by electrode mass or electrochemically active surface area, for example from the double-layer capacitance (McCrory et al., 2013), was not possible. The structural explanations above are therefore tentative, and the present results do not establish whether CF is intrinsically more effective than RVC or simply provides a larger active area per unit volume. CF was selected for the subsequent experiments because it gave the highest removal and is flexible, chemically stable and inexpensive.

The present results should be considered alongside earlier studies, while recognising the differences in their experimental approaches. Jha et al. (2012) achieved 97.79% tin leaching from waste solder using 4.5 M HCl at 90°C for 60 min. This value is consistent with dissolution from a solid material rather than electrodeposition from solution. Complexing compounds and their effect on the removal of metals by sodium trithiocarbonate precipitation was investigated by Thomas et al. (2018). In the present study the electrogenerative removal from prepared Sn(II) chloride solutions with CF and RVC cathodes is compared. These differences in feed composition, operating conditions and measured outcomes make it impossible to compare the reported percentages directly. The results show that removal is efficient under the conditions we studied, but we need to do more studies with complex waste solutions to see how useful it is in practice. CF and RVC are both carbon materials but their fibrous and open-cell structures are different. The comparison here is of the same flow-through configuration and not of superiority to other electrochemical recovery methods. Relative performance, energy requirements and product quality must be assessed by direct comparisons under matched conditions. (Table S1)

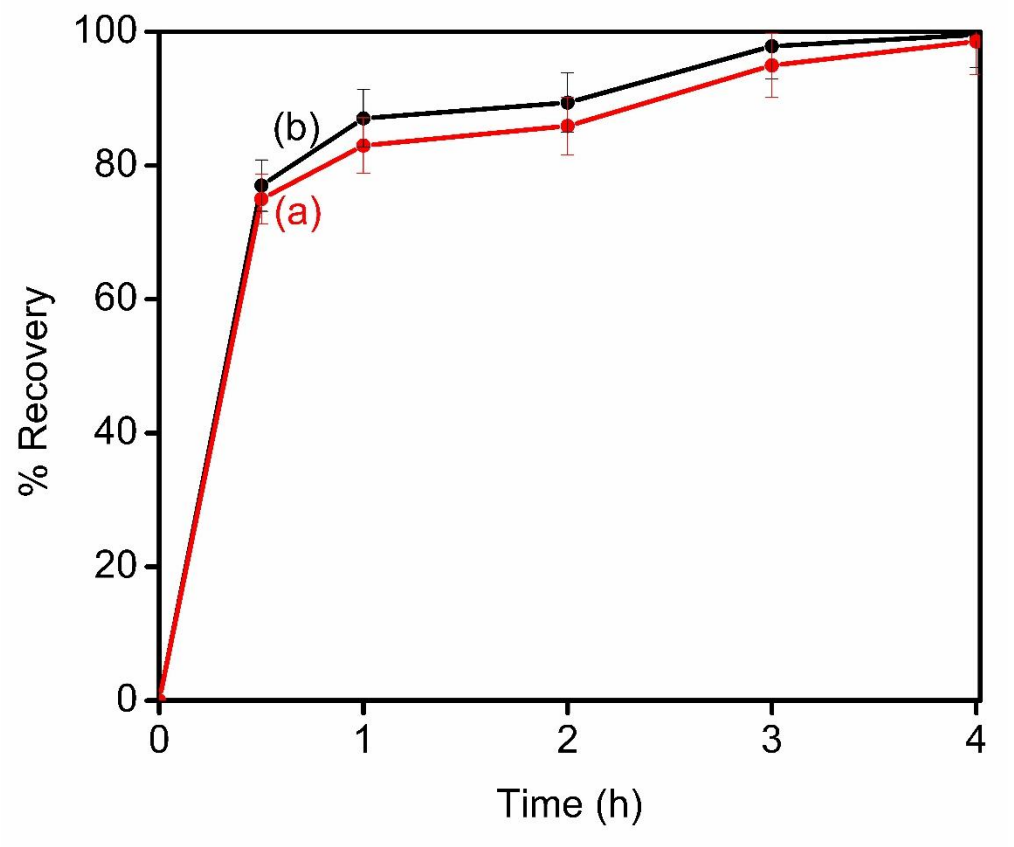


Figure 3. Removal of Sn(II) (500 mg L^{-1}, N_2 purging) with (a) RVC and (b) CF cathodes. Error bars: ±5 % of each value.

3.4 Effect of initial Sn(II) concentration

Various catholyte solutions with concentrations of 50, 100, 250, and 500 mg L^{-1} were used to investigate the effect of the initial Sn(II) concentration. The removal of Sn(II) with the CF cathode increased with the initial concentration over the range studied. Fig. 4 shows the percentage removal over time for each initial concentration.

For a process controlled entirely by mass transport, the removal rate is proportional to the bulk concentration, $r = (V_e/V_R)k_mA_eC_t$. The absolute rate therefore increases with C_0, whereas the fractional removal at a given time is independent of C_0. The larger absolute removal rates at higher C_0 are thus expected from the larger concentration driving force. The higher fractional removal at higher C_0, however, shows that the process was not controlled by

mass transport alone. Possible contributions include concentration-dependent nucleation and growth of the deposit, a fixed loss of Sn(II) by adsorption or precipitation that is proportionally larger at low C_0, and larger relative analytical uncertainty at low concentrations. Changes in conductivity are unlikely to explain the trend, because the supporting electrolyte dominates the ionic strength: even at 500 mg L^{-1}, $SnCl_2$ (4.2 mM) contributes only about 6 % of the total ionic strength. Using the apparent k_mA_e of CF (Section 3.6), the mass-transport-limited current, $I_L = nFk_mA_eV_eC$, is estimated as about 70 mA at 500 mg L^{-1} and 7 mA at 50 mg L^{-1}; direct current measurements would be required to determine how closely the cell approached these limits. (Table S2)

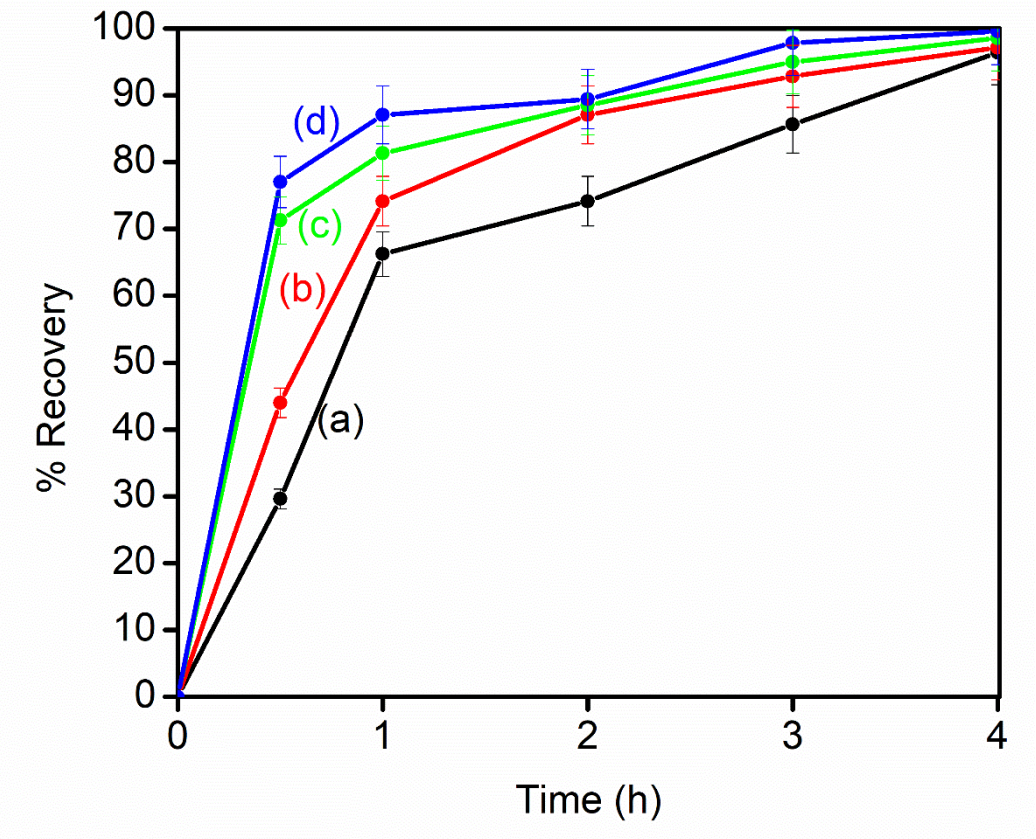


Figure 4. Effect of different initial concentrations of Sn(II) with (a) 50 mg L^{-1} Sn(II), (b) 100 mg L^{-1} Sn(II), (c) 250 mg L^{-1} Sn(II), and (d) 500 mg L^{-1} Sn(II) within 4 h of operation with CF as cathode.

3.5 Effect of oxygen

Dissolved oxygen had a marked effect on the removal of Sn(II). To minimise it, nitrogen gas was continuously bubbled through both the catholyte and anolyte during the experiments to reduce dissolved oxygen. As shown in Figure 5, the removal of Sn(II) with the carbon felt cathode at an initial concentration of 500 mg L^{-1} was markedly higher when nitrogen was purged. The removal after 4 h was 99.6 % with nitrogen purging but only 82.3 % without it, and the apparent pseudo-first-order rate constant decreased from 1.35 to 0.45 h^{-1} (Table 2). This continuous nitrogen purging was essential both before and during the electrochemical process to minimise dissolved oxygen in the solution. Improved recovery in the absence of oxygen has also been reported for electrogenerative gold recovery (Roslan et al., 2020). However, the mechanism in the present system remains uncertain. Competing oxygen reduction, oxidation of deposited tin, and changes in cathode potential are possible explanations, while nitrogen bubbling may also influence mixing and mass transport. Dissolved oxygen measurements, current profiles with and without Sn(II), and deposit characterisation under both conditions are needed to distinguish these effects. In any case, a threefold change in the rate constant caused by dissolved oxygen is not consistent with a process controlled by mass transport alone. (Table S3)

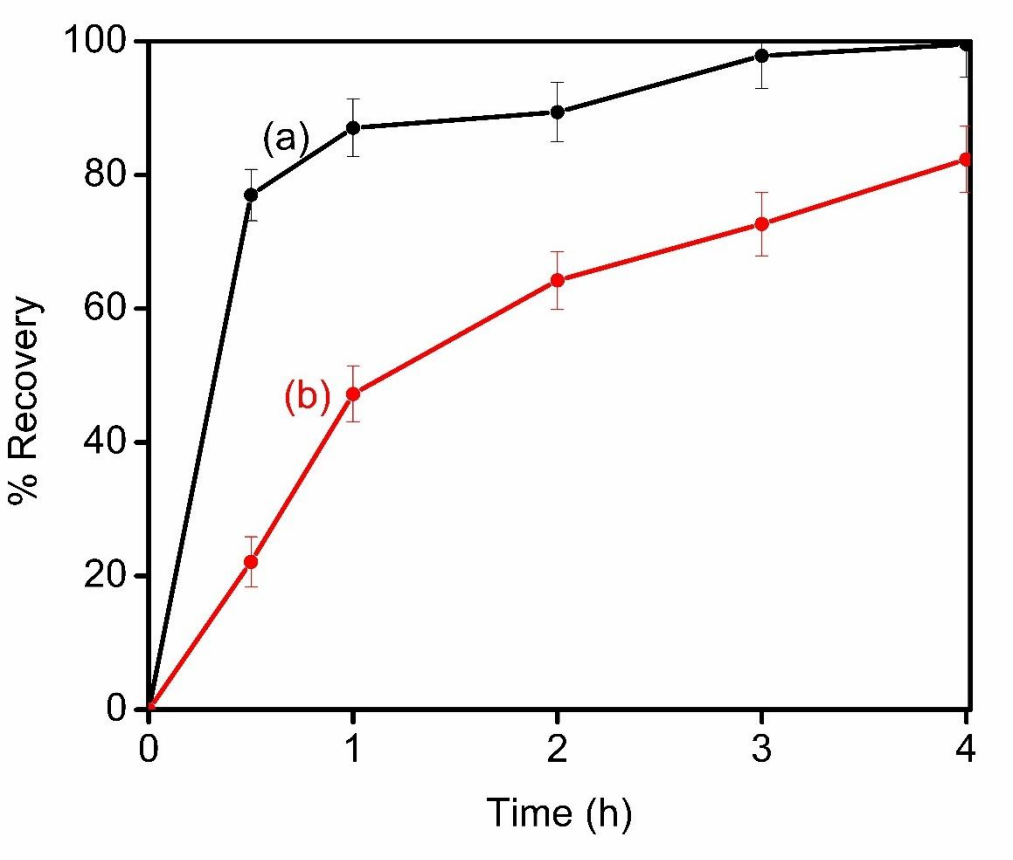


Figure 5. Effect of dissolved oxygen on Sn(II) removal (a) with and (b) without nitrogen purging (CF cathode, 500 mg L^{-1} Sn(II)). Error bars: ±5 % of each value.

3.6 Kinetic study

The concentration–time profiles for CF and RVC can be linked to the kinetic analysis of Sn(II) removal from dilute chloride solutions, as shown in Figure 6. For a batch-recirculation system in which the electrolyte passes through a porous three-dimensional cathode under complete mass-transport control and the conversion per pass is small, the concentration in the reservoir decays exponentially with time (Walsh, 2001):

$$ln\frac{C_t}{C_0} = -(\frac{V_e}{V_R})k_m A_e t \quad (6)$$

where V_e is the volume of the porous cathode (4.47 cm^3), V_R is the volume of catholyte in the recirculation loop, k_m is the mass-transfer coefficient, A_e is the specific surface area of the cathode (area per unit electrode volume), and C_0 and C_t are the Sn(II) concentrations at t =

0 and at time t. Because A_e was not measured, the product k_mA_e was obtained from the slope. Fig. 6 shows that the normalised Sn(II) concentration decreased throughout the 4 h experiments, and Fig. 7 shows the corresponding $\ln(C_t/C_0)$–t plots. A linear $\ln(C_t/C_0)$–t relationship corresponds to (pseudo-)first-order kinetics, whereas zero-order kinetics would require C_t itself to decrease linearly with time. The fitted parameters of both models are listed in Table 2.

The pseudo-first-order model described the data considerably better than the zero-order model for both cathodes (R^2 = 0.92 and 0.88 for CF and RVC, compared with 0.51 and 0.53 for a linear C_t–t fit; Table 2), so the earlier description of the process as zero order is not supported. The apparent rate constants were 1.35 h^{-1} for CF and 1.07 h^{-1} for RVC, corresponding to apparent k_mA_e values of 19.2 × 10^{-3} and 15.3 × 10^{-3} s^{-1}. A first order dependence on concentration is compatible with a large contribution of mass transport However, the $\ln(C_t/C_0)$–t plots are not strictly linear: the rate of decrease in the first 0.5 h was higher than the rate of decrease in the following 1.5 h and the steep final decrease is based on residual concentrations of only 2–7 mg L^{-1}, where small analytical errors produce large errors in the logarithm. Moreover, the rate constant was strongly dependent on dissolved oxygen (0.45 $^{h-1}$ without purging) and on pH (0.76–1.18 h^{-1} between pH 4 and 7), which would not be expected if mass transport were the only rate-limiting step. The fast initial decrease could also contain other contributions such as hydrolysis / precipitation of Sn(II) or adsorption on the cathode. The k_mA_e values should therefore be considered as apparent values describing the overall rate of Sn(II) removal. (Tables S4 & S5)

Table 2. Kinetic parameters for Sn(II) removal (500 mg L^{-1} Sn(II); fitted to the mean values of three runs).

Experiment	**Zero-order R^2**	**k_1 (h^{-1})**	**First-order R^2**	**Apparent k_mA_e (10^{-3} s^{-1})**
CF, N_2	0.51	1.35	0.92	19.2
RVC, N_2	0.53	1.07	0.88	15.3
CF, no N_2	0.88	0.45	0.97	6.4

CF, pH 4, N_2	0.82	0.76	0.96	10.8
CF, pH 5, N_2	0.72	0.91	0.96	13.0
CF, pH 7, N_2	0.50	1.18	0.87	16.8

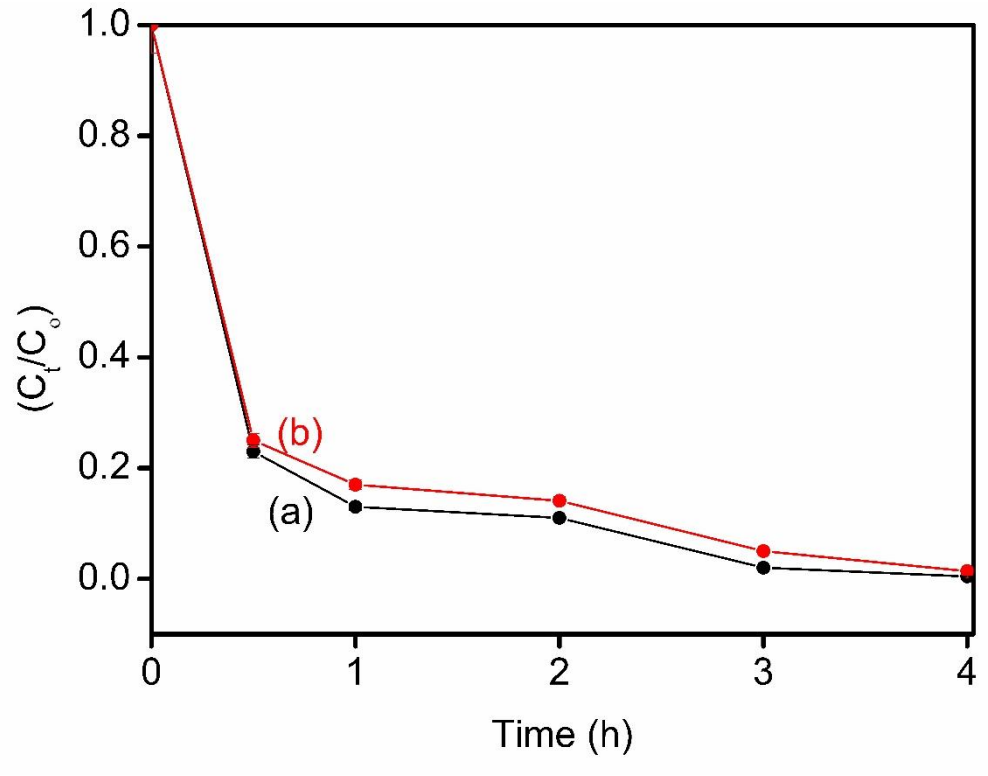


Figure 6. Normalised Sn(II) concentration, C_t/C_0, versus time for an initial Sn(II) concentration of 500 mg L^{-1} with (a) CF and (b) RVC cathodes.

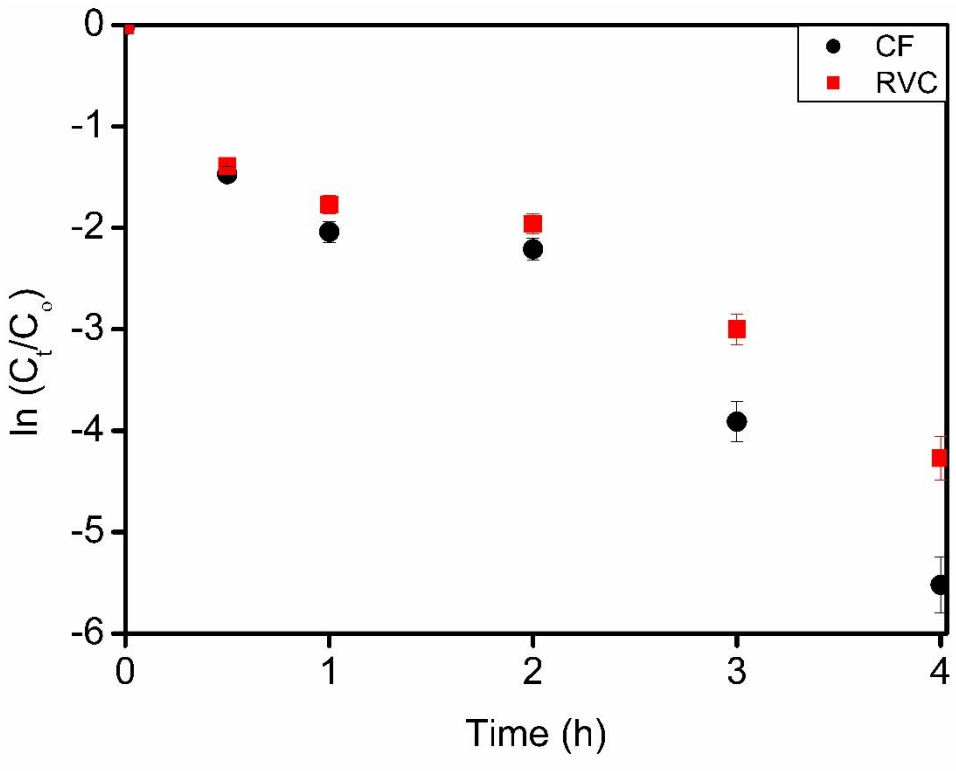


Figure 7. $\ln(C_t/C_0)$ versus time for an initial Sn(II) concentration of 500 mg L^{-1} with CF and RVC cathodes.

3.7 Influence of pH

The effect of catholyte pH was examined at pH 4, 5 and 7 with 500 mg L^{-1} Sn(II) and the CF cathode (Fig. 8), and without pH adjustment. The pH range was limited by Sn(II) chemistry: Sn(II) hydrolyses extensively and its hydroxide and oxide phases have low solubility near neutral pH, so precipitation becomes increasingly likely at and above pH 7, whereas at low pH hydrogen evolution competes increasingly with tin deposition (Séby et al., 2001; Cigala et al., 2012). After 4 h, the removal was 96.2, 96.9 and 99.2 % at pH 4, 5 and 7, respectively, and 97.1 % without pH adjustment (data not shown in Fig. 8). These final values differ by only about 3 percentage points, which is within the error bars. The main effect of pH was on the initial rate: the removal after 0.5 h increased from 29.6 % at pH 4 to 44.1 % at pH 5 and 75.4 % at pH 7, and the apparent rate constant increased from 0.76 to 1.18 h^{-1} (Table 2).

Under more acidic conditions (pH 4 and 5), a longer time was required to reach 90 % removal. This delay may be due to the competition between hydrogen ions and Sn(II) ions for active sites on the cathode surface, leading to proton reduction and potentially hindering tin deposition. Additionally, hydrogen gas evolution at lower pH levels may disrupt the electrode surface and promote chemical redissolution of the deposited tin.

The faster decrease of dissolved Sn(II) at pH 7 does not necessarily indicate greater deposition of metallic tin. Near neutral pH, hydrolysis, oxidation and precipitation may also lower the measured Sn(II) concentration, and the present measurements do not distinguish these contributions from electrodeposition. Because this also applies to the other experiments, which were all carried out at pH 7 (Section 2.1), the removal values reported in this work represent the overall decrease of dissolved Sn(II). Moreover, because only three controlled pH values were tested, the results indicate a trend within pH 4–7 rather than an optimum pH; measurements at intermediate and lower pH values, combined with a tin mass balance, would be needed to define the pH dependence of tin deposition more precisely. (Table S6)

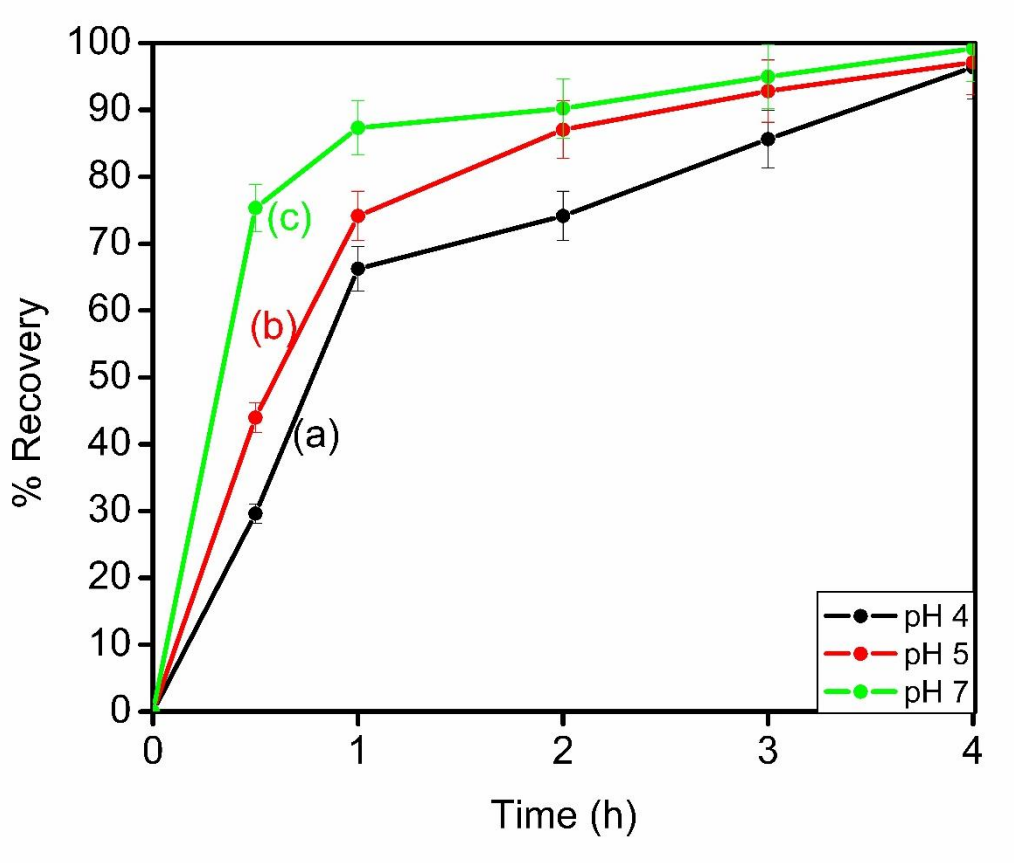


Figure 8. Removal of Sn(II) at different catholyte pH values (500 mg L^{-1} Sn(II), CF cathode, N_2 purging). Error bars: ±5 % of each value.

3.8 Morphology analysis

Fig. 9 shows SEM images of the CF cathode before (a) and after (b) a 4 h experiment. The pristine fibres (about 10 µm in diameter) are smooth, whereas after operation the felt is covered by a thick, cracked deposit that obscures the individual fibres. The two images were recorded at different magnifications (3000× and 500×, respectively), so they illustrate the formation of the deposit qualitatively but do not allow a quantitative comparison of the surface. After operation, the CF electrode also changed from black to greyish (Fig. 10).

These observations show that a solid deposit formed on the cathode. Morphology and colour alone, however, cannot establish the composition of the deposit, because tin oxides, hydroxides or hydroxychlorides could also form under the experimental conditions, particularly near neutral pH. Elemental mapping by energy-dispersive X-ray spectroscopy, X-

ray diffraction and X-ray photoelectron spectroscopy of the Sn 3d region would be required to confirm metallic tin and to distinguish it from Sn(II) and Sn(IV) species. The cracking of the deposit may be attributed to internal stress during growth or to hydrogen evolution, which is common in aqueous cathodic systems.

The present experiments do not establish how the system performs over repeated recovery and stripping cycles. Further testing is needed to assess whether recovery efficiency can be maintained, how readily the deposit can be removed from CF, and whether electrode changes, membrane fouling, increased flow resistance, or zinc-anode passivation affect operation. These measurements would provide a stronger basis for evaluating reusability and long-term stability.

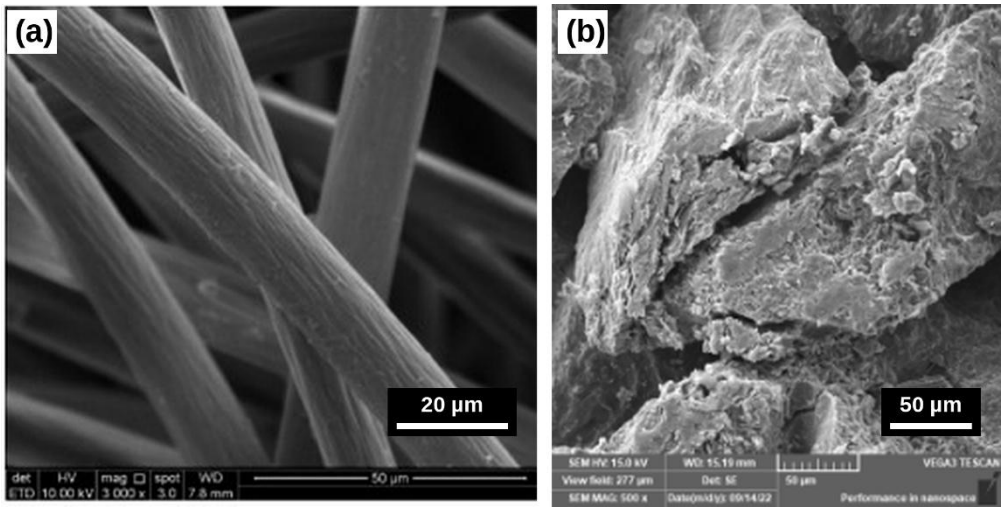


Figure 9. SEM micrographs of the CF cathode (a) before operation (3000×, 10 kV) and (b) after 4 h of operation with 500 mg L^{-1} Sn(II) (TESCAN VEGA 3, 500×, 15 kV). The enlarged scale bars were drawn to the scale of the original instrument scale bars, which are retained in the data bars.

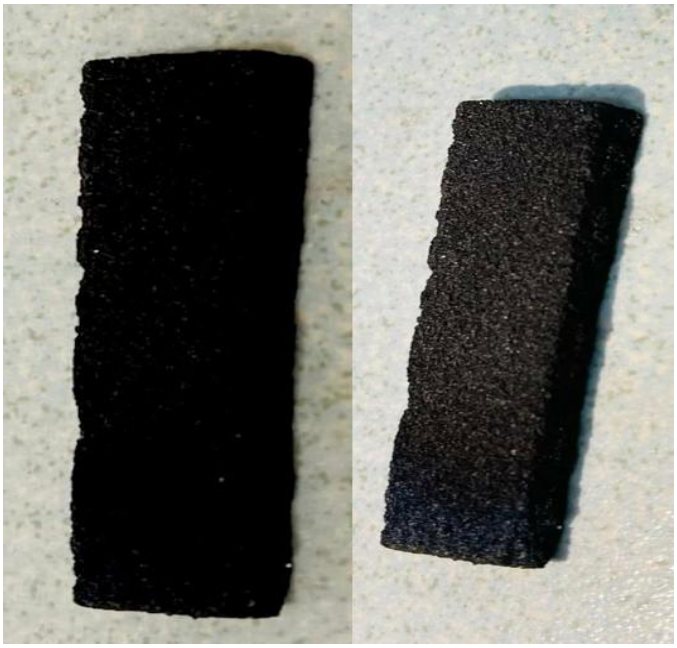


Figure 10. Photographs of the CF cathode before (left) and after (right) 4 h of operation with 500 mg L^{-1} Sn(II).

3.9 Limitations of the present study

The results of this study establish that dissolved Sn(II) was removed efficiently in the electrogenerative flow-through cell, but several quantities needed to characterise the process as tin recovery were not determined. First, the cell current was not recorded, so the charge passed and the faradaic efficiency of tin deposition are unknown (Section 3.1). Second, no tin and zinc mass balance was established: the tin deposited on the cathode, any precipitate, the tin retained in the cell and membrane, and the zinc dissolved from the anode were not quantified, so the fraction of the removed Sn(II) that was recovered as metal is unknown. Third, the composition and purity of the deposit were not determined (Section 3.8). Fourth, the validation parameters of the UV–vis method, such as the limits of detection and quantification and the effect of Zn(II), chloride complexation and pH, were not determined; the final residual concentrations (about 2–7 mg L^{-1}, corresponding to 99.6–98.6 % removal) should therefore be regarded as approximate. Fifth, the mass, real surface area, porosity and hydrodynamic resistance of the cathodes were not measured, which limits the comparison of CF and RVC (Section 3.3). Finally, no blank voltammogram was recorded, which limits the assignment of

some CV features (Section 3.2). These measurements are the priorities for further work and are required before conclusions can be drawn about the efficiency, product quality or practical applicability of the process.

4. Conclusion

The electrogenerative removal of Sn(II) from $SnCl_2$/NaCl solutions was studied in a flow-through reactor with CF and RVC cathodes and a zinc anode. Cyclic voltammetry on CF showed a cathodic wave with a peak at about -1.2 V and an anodic stripping peak at about -0.35 V vs. Ag/AgCl for 500 mg L^{-1} Sn(II), in agreement with Sn(II)/Sn(0) deposition and dissolution. After 4 h, the dissolved Sn(II) concentration decreased by 99.6% with CF and 98.6% with RVC at 500 mg L^{-1} Sn(II). CF provided slightly higher removal at all sampling times, but the differences were within the experimental scatter.

Increasing the initial Sn(II) concentration from 50 to 500 mg L^{-1} increased both the absolute and fractional removal. Purge with nitrogen was necessary, as without it only 82.3 % of the Sn(II) was removed after 4 h. Removal was quickest at pH 7, but ultimate removal varied only about 3 percentage points between pH 4 and 7. Hydrolysis and precipitation may account for some of the removal near neutral pH. The decay was pseudo-first-order rather than zero order in concentration. The strong effects of dissolved oxygen and pH indicate that the rate was not limited by mass transport only. SEM showed a cracked layer on the CF fibers.

The results show a first demonstration of Sn(II) removal from synthetic $SnCl_2$ /NaCl solutions using CF and RVC cathodes. Further work is required to ascertain if this performance can be maintained in more complex solutions. Tests with competing metals and different concentrations of chlorides and sulfates would help to assess the selectivity of tin, the recovery of metal and the purity of the deposit. The first priorities are to measure the cell current and faradaic efficiency, perform tin and zinc mass balances, and chemically identify the deposit.

Zinc consumption, energy requirements, and secondary waste must also be evaluated before any conclusions can be drawn about industrial applicability or sustainability. The deposit removal, electrode reusability and long-term system stability are also evaluated through repeated recovery and stripping tests.

Acknowledgement

The Tin Industry (Research and Development) Board, Ministry of Energy and Natural Resources Malaysia (304 / PKIMIA / 6501197), financially supported this study.

Data Availability Statement

All analysed data are included in this article. Raw data are available upon request.

Conflict of Interest

The authors declare that they have no conflicts of interest relevant to the work reported in this manuscript.

Declaration of artificial intelligence use

AI-assisted tools were used solely to improve writing clarity and check grammar during manuscript preparation. These tools were not used to generate data. All authors reviewed and approved the final manuscript and take full responsibility for its content, including the accuracy and integrity of the data presented.

References

Bard, A. J., & Faulkner, L. R. (2001). *Electrochemical methods: Fundamentals and applications* (2nd ed.). Wiley.

Cao, P., Liu, Y.-L., Zhang, Q., Guo, C., Li, J., & Zeng, Q. (2026). Advanced self-bias photocatalytic system for U(VI) and tetracycline hydrochloride removal coupled with electricity generation via

Ti_3C_2@$Cu_{1.96}S$/TiO_2-Si heterojunction. *Advanced Functional Materials, 36*(5), e14318. https://doi.org/10.1002/adfm.202514318

Chakrabarti, M. H., Brandon, N. P., Hajimolana, S. A., Tariq, F., Yufit, V., Hashim, M. A., Hussain, M. A., Low, C. T. J., & Aravind, P. V. (2014). Application of carbon materials in redox flow batteries. *Journal of Power Sources, 253*, 150–166. https://doi.org/10.1016/j.jpowsour.2013.12.038

Cigala, R. M., Crea, F., De Stefano, C., Lando, G., Milea, D., & Sammartano, S. (2012). The inorganic speciation of tin(II) in aqueous solution. *Geochimica et Cosmochimica Acta*. https://doi.org/10.1016/j.gca.2012.03.029

Flowers, P., Theopold, K., Langley, R., & Robinson, W. R. (2019). *Chemistry 2e*. OpenStax. https://openstax.org/details/books/chemistry-2e

Friedrich, J. M., Ponce-de-León, C., Reade, G. W., & Walsh, F. C. (2004). Reticulated vitreous carbon as an electrode material. *Journal of Electroanalytical Chemistry, 561*, 203–217. https://doi.org/10.1016/j.jelechem.2003.07.019

Jha, M. K., Choubey, P. K., Jha, A. K., Kumari, A., Lee, J.-C., Kumar, V., & Jeong, J. (2012). Leaching studies for tin recovery from waste e-scrap. *Waste Management, 32*(10), 1919–1925. https://doi.org/10.1016/j.wasman.2012.05.006

Kumar, M., Khan, M. A., Al-Othman, Z. A., & Choong, T. S. Y. (2013). Recent developments in ion-exchange membranes and their applications in electrochemical processes for in situ ion substitutions, separation and water splitting. *Progress in Polymer Science, 42*(3), 187–261. https://doi.org/10.1016/j.progpolymsci.2014.04.003

Le, T. X. H., Bechelany, M., & Cretin, M. (2017). Carbon felt-based electrodes for energy and environmental applications: A review. *Carbon, 122*, 564–591.

Liu, Y.-L., Cao, P., Zhang, Q., Guo, C., Li, J., & Zeng, Q. (2025). Solar-activated ZnS@MXene heterostructure for integrated radioactive wastewater treatment and energy harvesting. *Water Research, 286*, 124254. https://doi.org/10.1016/j.watres.2025.124254

Mansor, N., Mohamed, N., Mehamod, F. S., & Suah, F. B. M. (2019). Galvanic deposition of Pd^{2+} ions in chloride solution using three-dimensional electrodes. *Journal of Electroanalytical Chemistry, 838*, 23–32. https://doi.org/10.1016/j.jelechem.2019.02.014

McCrory, C. C. L., Jung, S., Peters, J. C., & Jaramillo, T. F. (2013). Benchmarking heterogeneous electrocatalysts for the oxygen evolution reaction. *Journal of the American Chemical Society, 135*(45), 16977–16987. https://doi.org/10.1021/ja407115p

Mohd Azhari, M. H. A., Nizar, S. A., Syed Yaacob, S. F. F., Abdul Latip, A. F., Megat Hanafiah, M. A. K., & Mohd Suah, F. B. (2024). Recovery of low concentration of tin from synthetic wastewater by using an electrogenerative process. *Malaysian Journal of Analytical Sciences, 28*(6), 1337–1348. https://mjas.analis.com.my/mjas/v28_n6/pdf/Mohd%20Azhari_28_6_8.pdf

Reijnders, L. (2016). Conserving functionality of relatively rare metals associated with steel life cycles: A review. *Journal of Cleaner Production, 131*, 76–96. https://doi.org/10.1016/j.jclepro.2015.09.080

Roslan, N. A., Suah, F. B. M., & Mohamed, N. (2020). Influence of different 3-D electrodes towards the performance of gold recovery by using an electrogenerative process. *Arabian Journal of Chemistry, 13*(1), 1440–1448. https://doi.org/10.1016/j.arabjc.2017.11.015

Roslan, N. A., Suah, F. B. M., Mohamed, N., & Ibrahim, P. (2017). The use of an electrogenerative process as a greener method for recovery of gold(III) from e-waste. *Separation and Purification Technology, 182*, 1–8. https://doi.org/10.1016/j.seppur.2017.03.032

Séby, F., Potin-Gautier, M., Giffaut, E., & Donard, O. F. X. (2001). A critical review of thermodynamic data for inorganic tin species. *Geochimica et Cosmochimica Acta, 65*(18), 3041–3053.

Thomas, M., Białecka, B., & Zdebik, D. (2018). Removal of copper, nickel and tin from model and real industrial wastewater using sodium trithiocarbonate: The negative impact of complexing compounds. *Archives of Environmental Protection, 44*(1), 33–47. https://doi.org/10.24425/aep.2018.123837

Tichter, T., & Marshall, A. T. (2022). Electrochemical characterisation of macroporous electrodes: Recent advances and hidden pitfalls. *Current Opinion in Electrochemistry, 34*, 101027. https://doi.org/10.1016/j.coelec.2022.101027

Walsh, F. C. (2001). Electrochemical technology for environmental treatment and clean energy conversion. *Pure and Applied Chemistry, 73*(12), 1819–1837. https://publications.iupac.org/pac/73/12/1819/index.html

Wang, F., Xu, S., Wang, N., Fujita, T., Ning, S., Wei, Y., & Wang, X. (2024). Precise target capture and the dynamic separation of Sn(IV) in highly acidic media by combining N and P donor covalent organic framework silica-based composite adsorbents. *Journal of Cleaner Production, 474*, 143596. https://doi.org/10.1016/j.jclepro.2024.143596

Wang, Y., Su, R., Tang, S., Zhang, M., & Guo, M. (2025). Refined bifunctional deep eutectic solvent for one-step selective indium and tin recovery from spent LCDs. *Environmental Research, 285*, 122400. https://doi.org/10.1016/j.envres.2025.122400

Zhang, Q., Guo, L., Zhang, Y., Cao, P., Liu, Y.-L., Wang, J., … Zeng, Q. (2026). Interface-optimized electrode in successive capacitive deionization for high-efficiency radioactive wastewater remediation. *Journal of Hazardous Materials, 502*, 141031. https://doi.org/10.1016/j.jhazmat.2026.141031